Auger Electron Angular Distributions from Surfaces: Direct Comparison with Isoenergetic Photoelectrons

LOUIS J. TERMINELLO* AND JOHN J. BARTON

Angular distribution patterns of Auger electrons and of photoelectrons from a Cu (001) surface were measured at the same electron kinetic energy. These measurements reveal that the low kinetic energy angular distributions for Cu Auger electrons and Cu $3p_{3/2}$ photoelectrons differ substantially. This direct comparison between the photoelectron and Auger electron angular distributions demonstrates that, in some circumstances, the Auger process produces a complicated source wave whose nature must be explored before Auger angular distributions can be used for surface structure analysis.

DURING THE PAST FEW YEARS Auger electron and photoelectron diffraction have become widely accepted and popular techniques for determining structures at single-crystal interfaces—particularly at surfaces (*1*). Interpretation of the angular- and energy-dependent electron emission data collected for these studies has been predicated on quantum self-interference of an ejected electron wave that can scatter from nearby atoms. However, Frank *et al.* (*2*) reported unexpected Auger electron angular distributions that, they argue, could not be explained within the conventional electron-scattering formalism. They proposed a controversial physical model to explain their results. Subsequently, numerous commentators (*3–6*) argued that the model proposed by Frank *et al.* cannot explain a large body of existing experimental results extending back to the 1940s, and they offered alternative explanations that depend on existing electron-scattering theory. In this report we present empirical evidence that the original model of Frank *et al.* cannot be correct and that also conflicts with the alternatives presented by the commentators.

From the single-crystal solids used in their study, Frank *et al.* observe Auger electron angular distributions with a great deal of structure and—owing to the known short escape depth of electrons in solids—one might expect to extract considerable information about the crystalline surface from these measurements. Indeed, previous work (*1*) would suggest that the largest contribution to the observed angular variation for Auger electron emission from atoms below the surface would be "forward scattering," the modulation of the electron intensity due to interference between an atomic-like electron wave and portions of that same wave that scatter ("focus") in passing through atoms on the path to the detector. To the extent that forward-scattering predominates, one expects increased intensity whenever atoms lie between the emitter and the detector. By working back from the points of high intensity, one obtains information on the positions of atoms surrounding the emitter. Surprisingly, for samples with known crystal structures, Frank *et al.* observed dips along interatomic axes.

To explain their unexpected results, Frank *et al.* devised a new model for electron propagation in a solid. The observed dips were attributed to "shadowing," a classical attenuation of electron intensity caused by putative inhomogeneous inelastic electron scattering. Rejecting this as a sudden denial of quantum mechanics, several commentators offered to explain the observed shadows with electron-scattering models that remain consistent with earlier observations of electron emission from solids. These include complex multiple electron scattering (*4*), strong energy dependence of Auger electron angular distributions at low emission energies (*5*), forward-scattering phase shifts near π leading to destructive interference, and even sample misalignment (*3*). We show that the dips observed by Frank *et al.* are real and that they are not caused by any of these purported effects.

Our study compares the $M_2M_{4,5}M_{4,5}$ and $M_3M_{4,5}M_{4,5}$ Auger electron angular distribution patterns (ADPs) to the same patterns for $3p$ photoelectrons from a clean Cu (001) crystal face. We use the same electron kinetic energies for both the primary photoelectron emission and the secondary Auger emission to identify whether any of the scattering effects cited above or "electron shadowing" are responsible for the phenomenon observed by Frank *et al.*

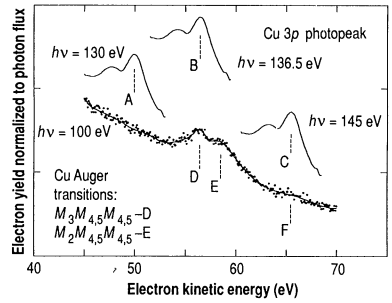

Fig. 1. A schematic that describes the Cu $3p$ photopeak and Auger electron kinetic energy positions used in this experiment. For point A the Cu $3p_{3/2}$ photopeak is at 51.8 eV. For point B the Cu $3p_{3/2}$ is at 56.6 eV, thus coinciding with the $M_3M_{4,5}M_{4,5}$ Auger peak. For point C the photopeak is at 65 eV. Features D and E are the $M_3M_{4,5}M_{4,5}$ and $M_2M_{4,5}M_{4,5}$ Cu Auger transitions taken at 100-eV photon energy (dots are actual data points and the line is provided to guide the eye). A measurement at point F has no Auger or photoelectron present and serves as a background (*9*).

Multiple-angle electron emission patterns were measured with an ellipsoidal mirror analyzer (*7*) operating as an electron energy band-pass filter while simultaneously preserving the angular distribution of the electrons ejected from the Cu sample. When used with monochromatized synchrotron radiation provided by beam line U8B at the National Synchrotron Light Source (*8*), we can place a photopeak at almost any relevant kinetic energy. This experimental setup allows us to make a direct comparison of an Auger and photoelectron angular distribution pattern at the same kinetic energy. Images were recorded with a video camera–digital histogramming system that permits optical thresholding and single-electron counting across the 80° acceptance cone (*9*).

The angle-integrated electron energy distribution curve obtained from a clean Cu (001) surface in Fig. 1 shows the energy position of the Cu $M_2M_{4,5}M_{4,5}$ and $M_3M_{4,5}M_{4,5}$ Auger electrons that are the focus of this study. Above that curve, the Cu $3p$ spin-orbit split photoelectron peak is shown schematically at three different energy positions relative to the constant-energy Auger electrons. Photoelectron angular distributions were measured at each of these three points indicated in Fig. 1. This placed the Cu $3p_{3/2}$ photopeak at a kinetic energy lower than, the same energy as, and an energy higher than the Cu Auger peaks. The Cu $M_2M_{4,5}M_{4,5}$ and $M_3M_{4,5}M_{4,5}$ Auger electron angular distributions were measured (without the Cu $3p$, or any other

IBM T. J. Watson Research Center, Yorktown Heights, NY 10598.

*Present address: Lawrence Livermore National Laboratory, Livermore, CA 94550.

photoelectron feature, in coincidence), thus permitting the comparison of the Auger electron and Cu core photoelectron ADPs at the same kinetic energy. The additional measurements allowed us to investigate the kinetic energy dependence of the Cu 3*p* and Auger electron angular distribution and draw conclusions regarding its importance. All Cu $3p_{3/2}$ and Auger electron ADPs taken under each of the conditions illustrated in Fig. 1 are shown in Fig. 2.

We first addressed whether the Auger electron dips along interatomic axes were reproducible in Cu (001). All of the atoms in our Cu (001) crystal below the first two layers have an atom directly above them; the model of Frank *et al.* would predict a dip in Auger electron intensity normal to the crystal surface. The pattern of electron emission at 56.6 eV from a clean Cu (001) surface illuminated by a 100-eV photon is shown in Fig. 2D. This energy corresponds to the Cu $M_3M_{4,5}M_{4,5}$ Auger electron peak, and a dip is observed. This result demonstrates that the dips observed by Frank *et al.* are not unique to their instrument, their sample, nor to the electron stimulation of the Auger electron current. However, our measurements do *not* substantiate their model for electron propagation as we show below.

We then studied whether the observed dip in the Auger electron emission patterns signal a breakdown in the existing models of electron scattering. One of the ideas implied or stated by the commentators cited above is that the lattice-scattering contribution of the Auger electron and photoelectron angular distributions should be identical if measured at the same electron kinetic energy: failure of any scattering model for Auger electron distributions would imply its failure for photoelectrons as well. The Cu 3*p* photoelectron angular distribution at 56.6 eV shows no dip (Fig. 2B). As illustrated in the inset to Fig. 2, a simple forward-scattering model would predict a peak in the normal emission direction. This peak is observed in the experimental results for photoelectrons at the same energy where the Auger emission shows no peak. This result demonstrates that the dips observed by Frank *et al.* are not caused by a complex multiple-scattering effect, nor by an unusually strong electron phase shift, nor by any kind of novel anisotropic inelastic electron scattering cross section. In fact, the dips are not caused by any scattering effect at all: the Auger and photoelectrons have the same energy and scatter from the same Cu atoms but have different angular distributions.

Finally we ask whether these results are specific to a particular electron kinetic energy. We have also measured the Cu 3*p* photopeak at 51.8 eV (below the Cu Auger peaks) and at 65 eV (above the Cu Auger peaks) (Fig. 2, A and C). Both of these cases show qualitatively similar images: the normal emission peak is predicted by a simple electron forward-scattering model and it is insensitive to energy. It has been argued (*4*, *5*) that forward-scattering models are inappropriate for the low kinetic energies at which our photoelectron ADPs are measured. However, a simplified, geometrical, forward-scattering model that would predict

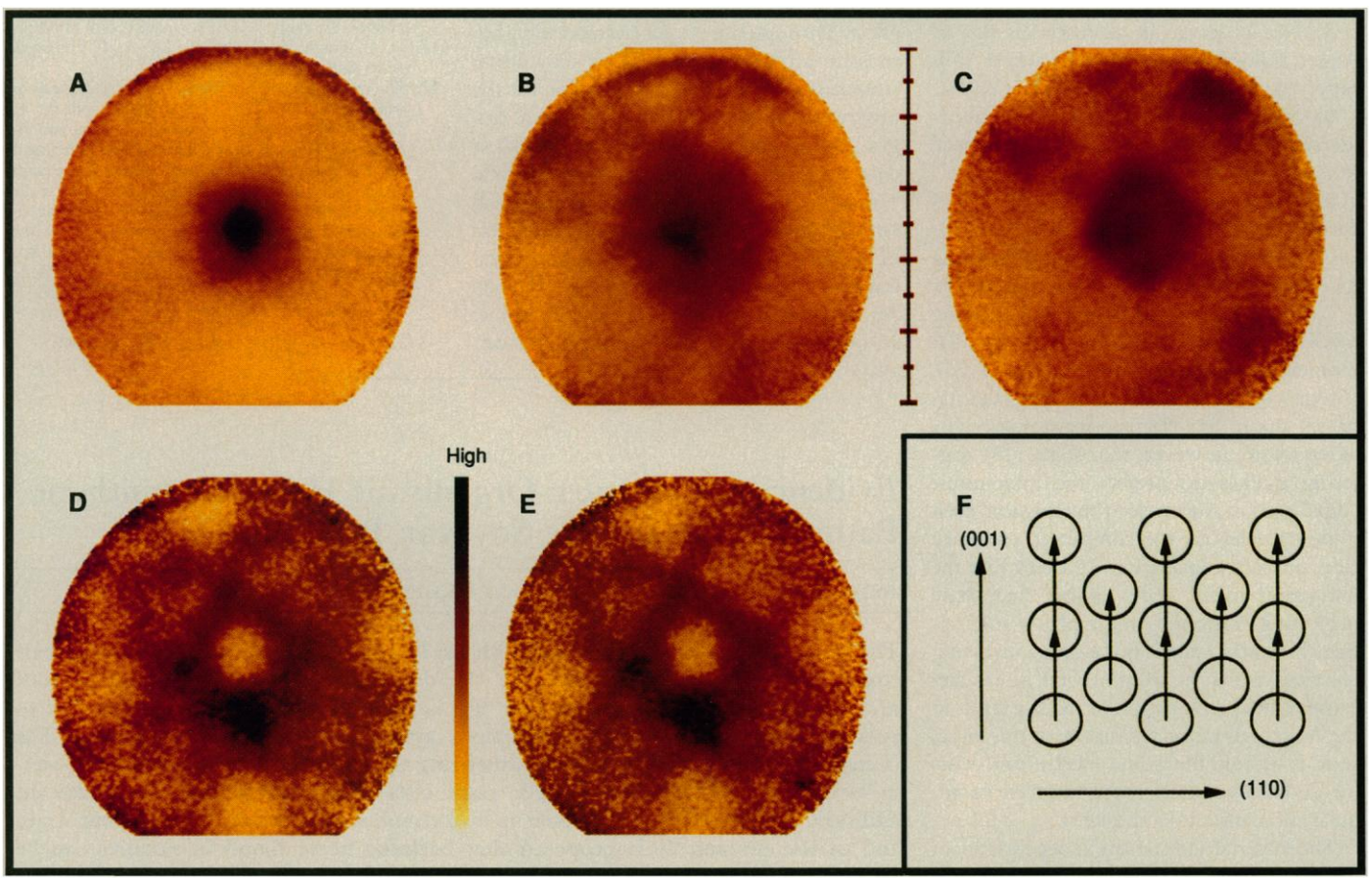

Fig. 2. These images (**A** to **C**) are the Cu $3p_{3/2}$ multiple angle photoelectron distribution patterns measured at points A, B, and C described in Fig. 1. Each image represents the angularly resolved electron emission from the Cu (001) surface with normal emission in the center of each image. For each Cu $3p_{3/2}$ image, normal emission has the greater intensity. The bottom two images are the Cu $M_3M_{4,5}M_{4,5}$ (**D**) and $M_2M_{4,5}M_{4,5}$ (**E**) Auger electron ADPs measured at points D and E in Fig. 1. Note the dip at normal emission in these images where the Cu $3p_{3/2}$ patterns had a maximum in intensity. The scale next to images B and C is proportional to the sine of the polar emission angle having 0° at the center. The inverse thermal scale used to represent the electron intensity is between panels D and E—for each pixel, the "darker" the color, the greater the electron intensity. (**F**) A cross section through the Cu (100) crystal with arrows indicating some of the forward-scattering paths that would lead to a peak along the normal emission direction.

an electron intensity peak along interatomic axes describes qualitatively the observed photoelectron normal emission intensity. Indeed, the Cu 3*p* photoelectron ADP at 56.6 eV is well described by a comprehensive multiple-scattering, spherical-wave simulation of the electron distribution (*10*). Similarly, the Auger electron ADP at 59 eV (Fig. 2E) shows an angular distribution nearly identical to the 56.6-eV image (Fig. 2D): the physical origin of the dip is not extraordinarily sensitive to electron energy.

What causes the dip in intensity along normal emission in the $M_{2,3}M_{4,5}M_{4,5}$ Cu Auger electron ADPs and—from the measurements of Frank *et al.* (*2*)—along interatomic axes in general? Any physical model must account for all electron angular distribution measurements from crystalline samples. To summarize, the interatomic axis, electron intensity dips are:

1) Observed in several different materials: Cu $M_{2,3}M_{4,5}M_{4,5}$ [(*11*) and this work], Pt *CVV* (*2*), and Ni $M_{2,3}M_{4,5}M_{4,5}$ (*11*).

2) Observed for Auger transitions considered to be "quasi-atomic" based upon their energies and linewidths (*12, 13*).

3) Not observed in all materials nor all Auger transitions in materials where it is observed: Al *LVV* (*11*) and Cu *LVV* (*14*).

4) Not observed in photoemission under identical conditions where they are observed in Auger emission (this work).

5) Not observed for atoms on top of surfaces (*2, 11*).

6) Not predicted by quantum-scattering models using *s*-wave continuum waves (*15*).

7) Predicted by quantum-scattering models in which higher (l = 3) angular momentum continuum waves are used (*16*).

Our work here eliminates any explanation based upon an electron-scattering effect alone. Note, however, that some (*16*) scattering models do predict the interatomic "dips" seen in Auger electron emission, even if these models are too complex to provide a clear physical explanation. It seems that the diffraction initial state (Auger final state neglecting scattering) must play a role: either this initial state is not atomic, involving coherent emission from several atoms because of the participation of valence levels in the Auger relaxation transition, or this initial state is atomic but some mechanism exists for destructive interference between its angular momentum components.

The material and transition dependence of the phenomenon can be explained if it only occurs for Auger transitions involving *d* orbital angular momentum levels or (more generally) partly delocalized valence electron levels that may participate in chemical bonds. The "quasi-atomic" nature of the Auger transitions and the partial success of theories containing only single-center emission at predicting the dips argue against a valence-level involvement, but allow the possibility that some strong, inherent emission anisotropy exists in the Auger electron intensity. Note that even if the Auger transition populates all magnetic sublevels equally in an atomic-like continuum wave and hence has isotropic emission intensity, each sublevel certainly has anisotropic phase.

What are the implications of our results for the use of Auger electrons for determining the structure of surfaces? The dips observed by Frank *et al.* are real: simple extensions of the scattering models successful for photoelectrons but which ignore the Auger transition details will not be useful for analyzing Auger angular distributions from some systems. However, these dips are not observed for all Auger transitions nor even all Auger transitions in the same material. The classical "shadowing" model used by Frank *et al.* cannot be used even as a simple heuristic, because it attributes the electron intensity attenuation, or dips, along interatomic axes that they observe to a scattering effect. Through our Auger electron and photoelectron comparison, we have shown that scattering effects are not responsible for the observed differences. Until the physical origin of this phenomenon is understood in detail and its sensitivity to nonstructural variables in the emission process checked, structures proposed solely from the analysis of Auger electron ADPs—such as the extraordinary atop adsorption of Ag atoms on Ag monolayers on Pt reported by Frank *et al.* (*17*)—should be independently verified.

REFERENCES AND NOTES

1. C. S. Fadley, in *Synchrotron Radiation Research: Advances in Surface Science*, R. Z. Bachrach, Ed. (Plenum, New York, 1990); W. F. Egelhoff, Jr., *Crit. Rev. Solid State Mater. Sci.* **16**, 213 (1990), and references therein.
2. D. G. Frank *et al.*, *Science* **247**, 182 (1990).
3. S. A. Chambers, *ibid.* **248**, 1129 (1990).
4. W. F. Egelhoff, Jr. *et al.*, *ibid.*, p. 1129.
5. X. D. Wang *et al.*, *ibid.*, p. 1129.
6. D. P. Woodruff, *ibid.*, 1131.
7. D. E. Eastman, J. J. Donelon, N. C. Hien, F. J. Himpsel, *Nucl. Instrum. Methods* **172**, 327 (1980).
8. F. J. Himpsel *et al.*, *Nucl. Instrum. Methods Phys. Res.* **222**, 107 (1984).
9. Electron ADPs were all normalized to a background image taken at 65-eV kinetic energy (100-eV photon energy) such that any Cu photopeaks are at lower or much higher kinetic energy and would not contribute to the background electron distribution pattern. This method of photopeak and Auger-peak background removal is analogous to background subtraction methods routinely applied to one-dimensional electron distribution data.
10. J. J. Barton, S. W. Robey, D. A. Shirley, *Phys. Rev. B* **34**, 778 (1986); L. J. Terminello and J. J. Barton, unpublished results.
11. D. Aberdam *et al.*, *Surf. Sci.* **71**, 279 (1978).
12. P. J. Feibelman and E. J. McGuire, *Phys. Rev. B* **15**, 3575 (1977).
13. L. I. Yin *et al.*, *Phys. Rev. A* **9**, 1070 (1974).
14. D. M. Zehner *et al.*, *Phys. Lett. A* **62**, 267 (1977).
15. H. L. Davis and T. Kaplan, *Solid State Commun.* **19**, 595 (1976).
16. R. N. Lindsay and C. G. Kinneburgh, *Surf. Sci.* **63**, 162 (1977); D. J. Friedman and C. S. Fadley, *J. Electron Spectrosc. Relat. Phenom.* **51**, 689 (1990).
17. D. G. Frank, T. Golden, F. Lu, A. T. Hubbard, *MRS Bull.* **15** (no. 5), 19 (1990).

18. We would like to acknowledge useful discussions with D. G. Frank, A. T. Hubbard, and W. F. Egelhoff. We thank C. Costas, J. Yurkas, and A. Marx for technical assistance with the experiment and are grateful to W. J. Joel for assistance with image processing. This work was conducted at the National Synchrotron Light Source, Brookhaven National Laboratory, which is supported by the Department of Energy (Division of Materials Sciences and Division of Chemical Sciences of Basic Energy Sciences) under contract no. DE-AC02-76CH0016.

13 November 1990; accepted 7 January 1991

Evidence for an Inter-Organismic Heme Biosynthetic Pathway in Symbiotic Soybean Root Nodules

INDU SANGWAN AND MARK R. O'BRIAN*

The successful symbiosis of soybean with *Bradyrhizobium japonicum* depends on their complex interactions, culminating in the development and maintenance of root nodules. A *B. japonicum* mutant defective in heme synthesis in culture was able to produce heme as a result of its symbiotic association with the soybean host. The bacterial mutant was incapable of synthesizing the committed heme precursor δ-aminolevulinic acid (ALA), but nodule plant cells formed ALA from glutamate. In addition, exogenous ALA was taken up by isolated nodule bacteria of the parent strain and of the mutant. It is proposed that bacterial heme found in nodules can be synthesized from plant ALA, hence segments of a single metabolic pathway are spatially separated into two organisms.

BRADYRHIZOBIUM JAPONICUM IS THE bacterial endosymbiont of soybean (*Glycine max*) that functions as a nitrogen-fixing organelle within cells of a plant organ called a root nodule. It has been suggested that the heme prosthetic group of leghemoglobin, a plant protein abundant in nodules, is a bacterial product (*1*), but the